

Brownian Dynamics of Colloidal Hard Spheres.

3. Extended Investigations at the Phase Transition Regime

W. Schaertl^{1,2}

Received July 22, 1994

The phase behavior of hard-sphere colloidal systems in the volume fraction regime $0.46 < \phi < 0.64$ has been studied in detail using a new and efficient algorithm to treat the nonanalytic interaction pair potential. In particular the influence of various initial configurations such as purely random and face-centered cubic (FCC) has been investigated, and former simulations have been extended toward much longer time scales. Thus, in the case of randomly initiated systems, crystallization could be suppressed for a comparably long time ($\approx 500\tau_R$, where τ_R is the structural relaxation time) where the system remained in a metastable glassy state. The concentration dependence of the long-time self-diffusion coefficients of these systems has been analyzed according to free volume theory (Doolittle equation). Numerical data fit excellently to the theoretical predictions, and the volume fraction of zero particle mobility was found close to the expected value of random close packing. In case of the FCC initiated systems, samples remained crystalline within the simulated evolution time of $\sim 500\tau_R$ if their volume fraction was above the predicted freezing transition $\phi_F = 0.494$, whereas at lower concentrations rapid melting into a fluidlike disordered state is observed. It should be noted that this algorithm, which neglects higher-order correlations, considering only direct pair interactions, nevertheless yields the correct hard-sphere crystallization phase behavior as predicted in the literature.

KEY WORDS: Brownian dynamics; hard spheres; phase transitions of hard-sphere systems.

1. INTRODUCTION

It is well known from both numerical⁽¹⁾ and experimental⁽²⁾ studies that hard-sphere systems exhibit a face-centered cubic (FCC) crystalline phase

¹ Institut für Physikalische Chemie, 55099 Mainz, Germany.

² Present address: ERATO Hashimoto Polymer Phasing Project, 15 Morimoto-Chyo, Shimogamo Sakyoku, Kyoto 606, Japan.

transition at a volume fraction regime far below the crystalline close-packed state ($\phi = 0.741$). This crystallization is based exclusively on entropic effects and was quantitatively investigated by Monte Carlo (MC) simulations in the pioneering work of Hoover and Ree.⁽¹⁾ Using a single-occupancy cell model and extensive calculations, the authors determined thermodynamic equilibrium properties (i.e., pressure and entropy) of the hard-sphere solid. Thus, they found an FCC freezing point at $\phi_F = 0.495$ and the corresponding melting point at $\phi_M = 0.545$. These findings have since been experimentally confirmed by Pusey and van Megen,⁽²⁾ using optical Bragg reflection while investigating the phase behavior of a hard-sphere colloidal system comprised of PMMA-latex spheres within a decalin/CS₂ mixture.

Recently we have presented a novel numerical algorithm for efficiently simulating systems of interacting Brownian hard spheres,^(3,4) which uses no constraints, contrary to the Hoover–Ree model, thus not considering any far-ranged position correlations explicitly. Our earlier calculations, which were based on purely random initial particle configurations, agreed well with predictions for the fluid^(5,6) and the glassy^(7,8) state; however, no crystallization was detected in the predicted regime. This failure might have arisen from the exclusion of many-body correlations, thereby enabling prior simulation experiments to predict random packing even for systems that should crystallize. To study this phenomenon of suppressed crystallization in more detail, the results presented here are based on an analysis of the concentration regime $0.46 < \phi < 0.64$, using random and, for the first time, FCC initial configurations. In addition, the evolution time of some of the simulated systems has been extended by a factor of 30 compared to the previous calculations^(3,4) to check the long-time stability of the metastable or equilibrated structures, respectively. In Section 2 we provide a short description of our algorithm, including the parameters used in the current simulations. Section 3 contains definitions of the numerical quantities which have been used to probe the phase transition behavior of our hard-sphere systems. In the last section the results of the new simulation runs are presented and discussed, emphasizing that, using a simple numerical technique without any constraints, as do former cell models,⁽¹⁾ it has been possible to reproduce both the correct FCC crystallization and glass transition phase behavior of colloidal hard-sphere systems.

2. SIMULATION PARAMETERS

The simulations implement periodic boundary conditions⁽⁹⁾ with $N = 864$ particles in the central cubic box. The algorithm proceeds as follows in each of the successive time steps of formal duration τ :

1. Each particle is moved the distance $(2D_0\tau)^{1/2}$ in one of the randomly chosen directions along each Cartesian axis ($\pm x$, $\pm y$, $\pm z$). D_0 is the Stokes-Einstein diffusion coefficient, which equals $4.4 \times 10^{-13} \text{ m}^2 \text{ sec}^{-1}$ for free Brownian motion of particles of hard-sphere radius $R = 0.5 \mu\text{m}$ in water at 20°C . (Here, it should be noted that the characteristic structural relaxation time of this system τ_R , given by R^2/D_0 ,⁽⁵⁾ equals 0.57 sec.)

2. Any particle overlap detected after the move is corrected by pairwise shifting the interfering particles until they just touch. Although this shift may cause secondary overlaps with other particles, this is ignored,⁽³⁾ and the next time step τ proceeds from the particle configurations obtained after these shifts.

The calculation time step was adjusted to 0.5 msec ($\approx 0.001\tau_R$) to allow finite calculation time while minimizing the erroneous effects of secondary particle overlaps. As discussed in more detail in previous publications,^(3,4) at high concentrations these secondary overlaps in the particle configurations cause a significant decrease of the effective particle volume fraction ϕ_{eff} due to the reduced distance of touching particles compared to the theoretical hard-sphere value $2R$. At the given calculation time step, this effect has to be taken into account at concentrations $\phi > 0.40$. The results obtained in this work are discussed in terms of their dependence on these reduced concentrations ϕ_{eff} , which, in contrast to our earlier work, where a simple formula had been given to calculate ϕ_{eff} from the number of overlapping particles and the mean (!) particle overlap distance,^(3,4) this time has been determined numerically exact using the reduced radius of each single (!) particle in case it should overlap with others. Concerning particles which exhibit overlaps with more than one neighboring particle, the largest overlap is used to calculate the reduced radius. Nevertheless, these reduced volume fractions agreed well with the values previously approximated using the mean particle overlap, thus verifying our former assumptions presented in ref. 3.

Generally, from one simulation run, 100 particle configurations are stored with time spacing $\Delta t = 0.1 \text{ sec}$, corresponding to $0.1/0.0005 = 200$ calculation cycles of formal calculation time step τ . The first configuration is stored after 2 sec of equilibration ($\approx 4\tau_R$), which has been proved, from our former calculations, to be sufficient to reach an equilibrated structure which will not change further within given evolution time. To check the long-time stability of the structures previously investigated for comparably short evolution times ($12 \text{ sec} \approx 21\tau_R$), a few long-time runs were performed for a evolution time totaling 282 sec ($\approx 500\tau_R$), where, in order to reduce the data amount without losing time resolution by the choice of a longer time spacing Δt , not the configurations, but only certain numerical

quantities characterizing the structure of 700 configurations with $\Delta t = 0.4$ sec have been stored as a function of time. A detailed description of these quantities will be given further below.

The theoretical volume fraction ϕ , defined as $NV_S V_{\text{box}}^{-1}$ (N is the number of spheres, V_S is the sphere volume $= 4/3\pi R^3$), is adjusted by selecting an adequate volume of the cubic box (V_{box}). Once again it should be noted that, as stated above, especially at high concentrations the effective volume fraction ϕ_{eff} may be significantly smaller than this theoretical ϕ , due to the secondary particle overlaps. As in the previous work, hydrodynamic interactions are totally neglected, due to insufficient calculation power; however, theoretical predictions⁽¹⁰⁾ suggest that hydrodynamic interactions should not influence the phase behavior of the colloidal system.

3. DEFINITIONS AND PHYSICAL INTERPRETATIONS OF CHARACTERISTIC NUMERICAL QUANTITIES

3.1. Short- and Long-Time Self-Diffusion Coefficients D_S and D_L

These quantities, which characterize the single-particle mobility and its time-scale dependence, may easily be determined from the single-particle mean-squared displacements. According to Einstein,⁽¹¹⁾ the time-dependent self-diffusion coefficient $D(\Delta t)$ is given by the following equation:

$$D(\Delta t) = \langle (\mathbf{r}_i(t + \Delta t) - \mathbf{r}_i(t))^2 \rangle_{i,t} / (6 \Delta t) \quad (1)$$

Using Eq. (1), the mean-squared displacement has been determined from two sets of configuration data with time spacing Δt , by ensemble and time averaging, respectively. $D(\Delta t = 0.1 \text{ sec} < \tau_R)$ is defined as the short-time diffusion coefficient D_S , whereas $D(\Delta t = 5 \text{ sec} \gg \tau_R)$ in the case of our system corresponds to the long-time diffusion coefficient D_L . As shown previously,⁽³⁾ $D(\Delta t)$ does not further decrease at time scales $\Delta t > 2 \text{ sec}$ ($\approx 4\tau_R$). D_S is a measure for the particle mobility while the particle stays within the regime of its next neighbors. D_L , on the other hand, characterizes the probability of the particle to escape from this cage of its next neighbors.⁽¹²⁾ Close to crystallization or the glass transition, structural relaxation of the system is slowing down by a few magnitudes, which corresponds to a vast persistence of the next-neighbor cages, and thus implies a dramatic decrease of the long-time particle mobility (i.e., smaller D_L). Further on, if the sample volume drops beyond a critical value, i.e., the particle concentration corresponding to very high concentrations, a close-packed state which, in case of glassy hard-sphere systems, should correspond to the

geometrical random close packing $\phi = 0.64$, is reached and the particle mobility should be frozen completely. Therefore systems at this concentration should exhibit zero long-time particle mobility. The critical slowing down of simple fluid systems has been analyzed previously in terms of so-called free-volume theories. Many examples are found in the literature.^(12,13)

In the case of the crystallization phase transition, the Lindemann criterion⁽¹⁴⁾ predicts a value $D_L/D_0 = 0.1$ at melting for samples without hydrodynamic interactions, thus providing a dynamical measure for this transition. As stated above, the hard-sphere crystallization should occur in the regime 0.495 (freezing) $< \phi < 0.545$ (melting) far beyond close packing.^(1,2) Thus, a certain amount of free volume is left to the central particle within the cage of its next neighbors (at $\phi = 0.545$, the next-neighbor distance of an FCC configuration is $1.11 \times 2R$, compared to $2R$ at close packing, whence D_S should not be affected nearly as strongly by the FCC crystalline phase transition as D_L).

3.2. Structural Static Properties

As in previous work,⁽⁴⁾ the pair distribution $G_2(r)$ is used to characterize the structure of the simulated systems. In addition, a set of other quantities, used before in the error and convergence analysis of the algorithm,⁽³⁾ this time is applied to the structure analysis of the configurations:

As our hard-sphere system, with increasing ϕ_{eff} , tends toward a close-packed state, numerical quantities such as the number of touching (or slightly overlapping!) spheres $N(\tau)$, the number of particle pair contacts $ov(\tau)$, and the mean overlapping distance $d(\tau)$, all of these determined regarding the secondary overlaps after (!) the primary overlap corrections,⁽³⁾ are also expected to increase. On the contrary, $N(\tau)/ov(\tau)$, a measure for the cluster formation as well as the number of next neighbors with close contact, should decrease [$N(\tau)/ov(\tau) = 2$ for isolated pairs, 0.33 at FCC close (!) packing, and ~ 0.40 at random close packing]. However, in case of the FCC crystallization which occurs at $\phi_{\text{eff}} \approx 0.50$ far beyond crystalline close packing, $N(\tau)$, $ov(\tau)$, and $d(\tau)$ should be expected to decrease with increasing ϕ_{eff} ($\phi_{\text{eff}} > 0.50$), while $N(\tau)/ov(\tau)$ should increase. This can easily be deduced from the fact that the hard-sphere FCC crystal exhibits, compared to the fluid state at slightly lower particle concentration, a strongly increased tendency of particles toward staying at their sites defined by the initial FCC lattice and thus well separated from each other (i.e., less close-packed). Taking this into account, it should be possible to probe the crystalline phase transition of hard-sphere systems by investigating the above numerical quantities determined from the particle configurations.

It should be emphasized that, whereas the dynamical physical quantities discussed in Section 3.1 above as well as $G_2(r)$ can also be determined experimentally for colloidal hard-sphere systems, using, for example, dynamic light scattering (D_S, D_L)^(15,16) and SAXS [$S(q) \Rightarrow G_2(r)$],^(17,18) there is no experimental technique currently available which can measure quantities such as $N(\tau)/ov(\tau)$ directly. Digital image processing in connection with ultramicroscopy of core-shell systems^(19,20) may provide a future possibility to measure time-dependent configuration data of a colloidal hard-sphere system, thereby offering experimental access to quantities like the mean number of touching next neighbors or the accurate percentage of particle contacts within a given sample.

4. RESULTS AND DISCUSSIONS

Figure 1 shows the resulting $N(\tau)/ov(\tau)$ for long-time runs ($t \approx 500\tau_R$) of FCC (≈ 1.46) and randomly (≈ 1.17) initiated systems at effective volume fractions ≈ 0.54 , i.e., in the predicted limit of the existence of hard-sphere crystals.⁽¹²⁾ As stated above, these runs have been performed to check the long-time stability of the obtained structures, respectively, within the present technical limits. So, for example, one run of 864 particles at $\phi = 0.55$ with equilibration of 2 sec and evolution time of 280 sec took about 4 days on a Macintosh Quadra 840 AV (which is about ten times faster than the Macintosh II vx or Micro VAX 3000 used in our previous simulations^(3,4)). An application of our new efficient algorithm⁽³⁾ using

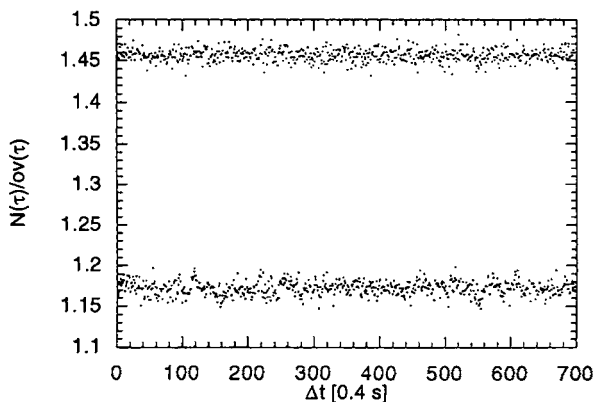


Fig. 1. Long-time stability of randomly [lower dots, $N(\tau)/ov(\tau) \approx 1.17$] and FCC [upper dots, $N(\tau)/ov(\tau) \approx 1.46$] initiated systems with $\phi_{\text{eff}} \approx 0.54$. The numerical quantity $N(\tau)/ov(\tau)$ is a measure for the close packing of the structure (see text). No significant changes of either system can be found within the simulated evolution time.

modern supercomputers should allow for a vast extension of the above time scale toward probably longer than $10,000\tau_R$.^(21,22) At present, our results show that in both cases the structure remains unchanged in the regime $(0-500)\tau_R$ after an equilibration of $4\tau_R$.

It should be noted that $N(\tau)/ov(\tau)$ is significantly larger in the case of the FCC initiated system, although both FCC and randomly initiated runs have treated comparable particle volume fractions. As stated before and will be discussed in more detail below [see Section 3.2 and comments on Fig. 6 below for a detailed discussion of the possibility to probe hard-sphere crystallization using the parameter $N(\tau)/ov(\tau)$], this increased $N(\tau)/ov(\tau)$ shows the tendency toward partial conservation of the initial crystalline order. Here, it should be mentioned that a perfect FCC crystal at volume fractions far beyond close packing should exhibit $N(\tau)/ov(\tau) = 0$. The above numerical result [Fig. 1, $N(\tau)/ov(\tau) \approx 1.46$] may be interpreted as follows: although on average staying at their well-defined lattice sites of the FCC state, the particles are continuously probing the walls of their cages, thus causing some particle contacts between next neighbors. Therefore, as deduced from the numerical results presented in this paper, the hard-sphere FCC crystalline state beyond close packing seems to be somehow fluctuating and distorted and not perfectly static and crystalline.

The rapid equilibration of both runs (≤ 2 sec) once more underlines the efficiency of the new technique. The lack of crystallization of the randomly initiated system may be explained by the very slow particle mobility and corresponding structural relaxation. Here, it should be noted that the experimentally observed time scale for crystallization is of the order of hours to days,⁽²⁾ and thus is much longer than the evolution time regarded in the present calculations. Concerning the FCC initiated system, it seems to be surprising that, although our algorithm is based only on direct pair interactions and neglects higher-order particle correlations,⁽¹⁾ the (distorted) equilibrium crystalline structure remains unchanged during the whole time regime $(0-500)\tau_R$. After having verified the long-time stability of the high-density amorphous (fluid-glassy) and crystalline (FCC-distorted) systems obtained from numerical calculations, the corresponding phase transition behavior (glass transition and crystallization) will be discussed in detail in the following.

4.1. Glass Transition of Monodisperse Hard Spheres

Our results concerning the random close-packing volume fraction, which might be identified with the glassy state of zero particle mobility, were determined earlier by analyzing the percentage of touching spheres and are published elsewhere.⁽⁴⁾ Whereas in these earlier investigations only

structural geometrical properties had been used to identify the glass transition, here an analysis based on the long-time particle mobility $D_L(\phi_{\text{eff}})/D_0$ will be presented. It is well known that the critical slowing down of the diffusivity in simple liquids may be interpreted in terms of the so-called free-volume theory. Only the basic equation to analyze our numerical results is given in this paper, as follows (for details see the numerous publications on this subject)^(13,23,24):

$$D_L(\phi_{\text{eff}})/D_0 = \exp[-c/(V - V_0)] \quad (2)$$

c here will be regarded as without special physical meaning concerning the glass transition, whereas V_0 corresponds to the volume V of samples without any free volume and, consequently, with zero particle mobility. In the case of hard spheres, therefore, V_0 should correspond to the volume which is occupied by a random close-packed system. Figure 2 shows the analysis of the long-time diffusivity of the amorphous dense systems in the concentration regime $0.54 \leq \phi_{\text{eff}} \leq 0.59$ according to Eq. (2). Here, the effective volume V of the systems has been calculated from ϕ_{eff} , using the simple relationship

$$V = NV_s/\phi_{\text{eff}} \quad (3)$$

N is the number of spheres ($=864$) and V_s the volume of one single sphere ($\frac{4}{3}\pi R^3 = 0.5236 \mu\text{m}^3$). As can be seen from Fig. 2, the numerical data agree very well with the theoretical predictions. The volume of random close

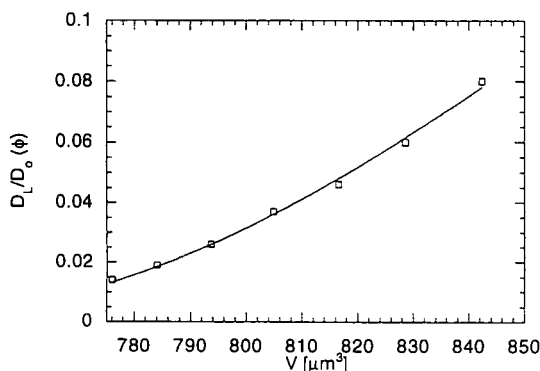


Fig. 2. Analysis of the concentration dependence of the long-time self diffusion coefficient [$D_L(\phi_{\text{eff}})$, symbols] of the amorphous systems by free-volume theory (Doolittle equation, line). Numerical data agree well with the theoretical fitting function, which predicts a zero-mobility limit of $\phi_{\text{eff}} \approx 0.66$, slightly shifted compared to the expected value $\phi_{\text{eff}} = 0.64$.

packing obtained from the fit corresponds to a volume fraction of 0.66, which is slightly larger than the theoretical value of 0.64. This finding may be explained by the fact that secondary particle overlaps are not identical in magnitude for all particles of the sample. Thus, a small effective size polydispersity is inflicted on the sample, which, as found before,⁽⁴⁾ shifts the regime of random close packing and the glass transition toward higher volume fractions. The value of 0.66 for ϕ_{RCP} would correspond to a radius polydispersity of $\sim 5\%$ if one assumes a Gaussian distribution of particle radii.⁽⁴⁾ This agrees well with the size profiles which have been obtained from numerical determination of the effective radius of each particle (Section 2) for our amorphous systems in the concentration regime $0.54 \leq \phi_{\text{eff}} \leq 0.59$.

4.2. Crystallization of Hard Spheres

Figure 3 illustrates the dependence of D_S and D_L on ϕ_{eff} in the hard-sphere volume fraction regime $0.46 < \phi_{\text{eff}} < 0.67$. Whereas the short-time behavior shows no significant difference between randomly and FCC initiated simulation runs, $D_L(\text{FCC})$ starts to deviate strongly from the fluid-state behavior at $\phi_{\text{eff}} \geq 0.495$, which therefore is identified with the freezing concentration. The largest difference between FCC and randomly initiated runs is reached at $\phi_{\text{eff}} \approx 0.54$, the melting concentration. At higher volume fractions, the long-time particle mobility converges again, indicating the transition to a close-packed state at $\phi_{\text{eff}} \approx 0.66$.

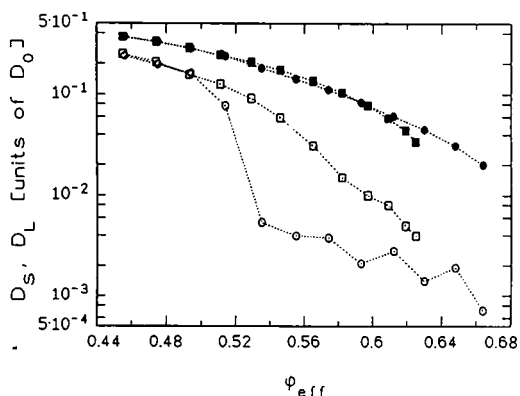


Fig. 3. Concentration dependence of short-time (D_S , filled symbols) and long-time (D_L , open symbols) self-diffusion coefficients from simulation runs with random (squares) and FCC (circles) initial configurations. FCC initiated systems exhibit distinct deviations from the fluid-state behavior at $\phi_{\text{eff}} \geq 0.495$, indicating the FCC crystallization of hard-sphere systems.

Figure 4 depicts the time-dependent self-diffusion coefficient for the fluid and crystalline states. As stated above, the particle mobility of the crystalline state diverges strongly in the long-time regime ($\Delta t \geq 2$ sec), whereas at shorter time scales ($\Delta t \leq 0.5$ sec) comparable particle diffusivity is obtained for the fluid and crystalline systems. It should be noted that a constant long-time limit D_L is maintained at $\Delta t \geq 2.0$ sec. Thus, our previous definition of D_L [$=D(\Delta t = 5 \text{ sec})$] corresponds well to the limit of infinite diffusion time.

In Fig. 5, $G_2(r)$ is presented for the volume fraction regime where FCC crystallization should occur [$\phi = 0.54$, $\phi_{\text{eff}}(\text{randomly initiated}) = 0.529$, $\phi_{\text{eff}}(\text{FCC}) = 0.535$]. The difference in ϕ_{eff} of randomly and FCC initiated systems is caused by the closer-packed equilibrium configuration of the randomly initiated run, resulting in more prominent secondary particle overlaps and correspondingly larger reduction of ϕ . Whereas at $\phi_{\text{eff}} \leq 0.50$ the results for both initial configurations correspond very well to the predictions of the Percus–Yevick approximation for the fluid state of hard-sphere systems,^(4,6) we find distinct differences in the regime $\phi_{\text{eff}} \geq 0.50$ (Fig. 5). The $G_2(r)$ of the FCC initialized system shows additional peaks corresponding to a (disordered) FCC crystal. At this point, we should mention that the tendency to maintain the initial perfect FCC structure increases with increasing $\phi_{\text{eff}} \geq 0.50$. No amorphous-state glass transition was found for FCC initiated systems at $\phi_{\text{eff}} \geq 0.58$ as predicted in the literature^(7,8) for randomly initiated and rapidly compressed systems. The reason may be that single-particle dynamics is too slow at these high

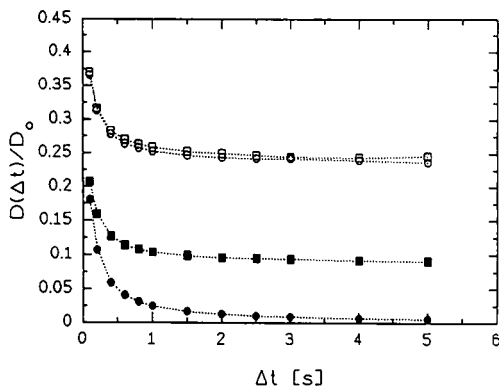


Fig. 4. Time-dependent self-diffusion coefficient $D(\Delta t)/D_0$ for fluid [$\phi_{\text{eff}}(\text{random}) = \phi_{\text{eff}}(\text{FCC}) = 0.456$ (open circles, squares), $\phi_{\text{eff}}(\text{random}) = 0.529$ (filled squares)] and crystalline [$\phi_{\text{eff}}(\text{FCC}) = 0.535$ (filled circles)] systems. The crystalline state shows distinct deviations of $D(\Delta t)/D_0$ (compared to the fluid state) which increase strongly with Δt , approaching the long-time limit at $\Delta t \approx 2$ sec.

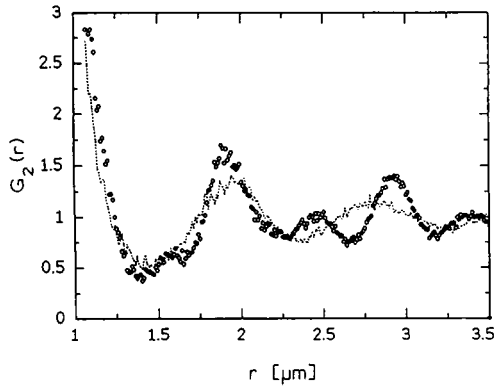


Fig. 5. Pair distribution function $G_2(r)$ for systems with random (dotted line) and FCC (circles) initial configurations. Given are results at $\phi = 0.54$, where $\phi_{eff}(\text{random}) = 0.529$ and $\phi_{eff}(\text{FCC}) = 0.535$. The data give evidence for the existence of a (distorted) FCC structure at $\phi_{eff} \geq 0.50$.

concentrations to reach the state of random close packing from FCC initial positions within the limited time of our simulations ($282 \text{ sec} \approx 500\tau_R$). As stated above, the same explanation could be valid in the case of the lack of crystallization of randomly initiated systems in the regime $0.50 \leq \phi_{eff} \leq 0.58$.

Finally, the concentration dependence of the equilibrium structure of our system can be characterized by the various quantities used in our

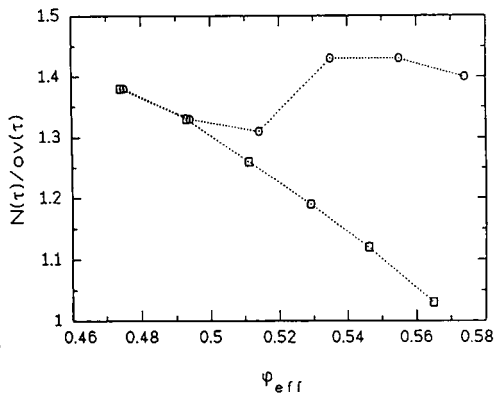


Fig. 6. Concentration dependence of $N(\tau)/ov(\tau)$ for systems with random (squares) and FCC (circles) initial configurations. FCC initiated systems at $\phi_{eff} \geq 0.496$ show less tendency toward cluster formation and close packing, thus giving evidence for a crystal-like structure with well-separated particles, isolated on defined lattice sites.

former error and convergence analysis of the algorithm⁽³⁾ and given in Section 3. Since all of these exhibit the FCC crystalline phase transition, here only $N(\tau)/ov(\tau)$ (Fig. 6) will be presented and discussed. Whereas the randomly initiated systems behave as anticipated for the amorphous fluid state (Section 3), the FCC initialized systems show decreasing tendency toward close packing at $\phi_{\text{eff}} \geq 0.50$ (freezing volume fraction!) with increasing ϕ_{eff} . This corresponds, as stated above, to an increased probability of the particles remaining at their initial FCC lattice sites. $N(\tau)/ov(\tau)$ reaches its maximum (~ 1.46) at $\phi_{\text{eff}} \approx 0.54$ which therefore might be identified with the hard-sphere melting volume fraction.

5. CONCLUSIONS

By extending former calculations to much longer time scales and using both random and FCC initial configurations, we have investigated the phase transition regime of colloidal hard spheres in more detail.

At high concentrations $\phi_{\text{eff}} \geq 0.50$, amorphous systems were obtained from random initialization, which did not crystallize within an evolution time of $\sim 500\tau_R$ although crystallization should be expected.^(1,2) It has been concluded that these kinds of metastable fluid- to glasslike amorphous dense states are maintained due to very slow structural relaxation, thus affording much longer evolution times for the samples to crystallize (the order of hours, as observed in real experiments^{(2)!}) than used in our simulations (~ 5 min). Free-volume theory⁽¹³⁾ has been used to analyze the concentration-dependent long-time diffusivity $D_L(\phi_{\text{eff}})$ of these amorphous systems, yielding as limit of zero particle mobility the theoretically expected concentration, i.e., the volume fraction of random close packing. A minor deviation toward too high volume fraction could be explained in terms of a slight polydispersity introduced to the effective particle radii by non-uniform secondary particle overlaps. As shown in our earlier work,⁽⁴⁾ polydispersity causes the volume fraction of random close packing to be shifted toward higher volume fractions.

Contrary to the above findings, starting from a well-defined crystalline FCC lattice, the crystalline order was largely maintained for time scales up to $500\tau_R$ in the regime $\phi_{\text{eff}} \geq 0.50$, without any indication of melting, i.e., complete disordering. Nevertheless, it might be possible that these crystalline systems melt at much longer time scales $t \gg 500\tau_R$ which cannot be investigated within reasonable calculation time on currently available computers. The crystallization, i.e., maintaining of the crystalline initial structure, could be probed using both dynamical and structural measures. The findings indicated the existence of a distorted but nevertheless crystalline structure with critically slowed down long-time diffusivity corresponding to

an effective caging of central particles by their next neighbors. As shown by the concentration dependence of the short-time diffusion coefficient D_S for both fluid-glassy and fluid-crystalline systems, the crystallization transition cannot be probed by this quantity. This may be understood from the fact that at crystallization in the regime $\phi_{\text{eff}} \geq 0.50$ a considerably large amount of free volume is left within the next-neighbor cages, thus imposing much less restriction on the particle motion within the length scale of the cage dimensions (D_S) than on the probability of particles to escape their cages (D_L). The results presented in this paper correspond very well to earlier findings concerning the crystalline phase transition of hard-sphere systems.^(1,2) At the very end it should be emphasized that our numerical technique, which is based on a very simple principle and uses neither constraints nor many-body correlations, nevertheless is adequate for investigating the complete phase behavior of colloidal hard-sphere systems.

ACKNOWLEDGMENTS

The author would like to thank H. Löwen, I. Moriguchi, T. Kawakatsu, and T. Odagaki for helpful discussions. This work has been partially supported by a grant from the Stipendienfonds der Deutschen Chemischen Industrie. Also some financial support from the Japanese Research and Development Corporation is gratefully acknowledged.

REFERENCES

1. W. G. Hoover and F. H. Ree, *J. Chem. Phys.* **49**:3609 (1968).
2. P. N. Pusey and W. van Meegen, *Nature* **320**:340 (1968).
3. W. Schaertl and H. Sillescu, *J. Stat. Phys.* **74**:687 (1994).
4. W. Schaertl and H. Sillescu, *J. Stat. Phys.*, to appear.
5. B. Cichocki and K. Hinsen, *Physica A* **187**:133 (1992).
6. G. Throop and R. J. Bearman, *J. Chem. Phys.* **42**:2408 (1965).
7. L. V. Woodcock, *J. Chem. Soc. Faraday II* **72**:1667 (1976).
8. L. V. Woodcock, *Ann. N. Y. Acad. Sci.* **371**:274 (1981).
9. H. Gould and J. Tobochnik, *An Introduction to Computer Simulations*, Parts 1 and 2 (Addison-Wesley, 1988).
10. M. Medina-Noyola, *Phys. Rev. Lett.* **60**:2705 (1988).
11. A. Einstein, *Ann. Phys.* **17**:549 (1905).
12. Y. Hiwatari, H. Miyagawa, and T. Odagaki, *Solid State Ionics* **47**:179 (1991), and references therein.
13. A. K. Doolittle, *J. Appl. Phys.* **22**:1471 (1951).
14. H. Löwen, Private communication.
15. W. van Meegen and S. M. Underwood, *J. Chem. Phys.* **91**:552 (1989).
16. E. Bartsch, M. Antonietti, W. Schupp, and H. Sillescu, *J. Chem. Phys.* **97**:3950 (1992).
17. E. B. Sirota, H. D. Ou-Yang, S. U. Sinka, P. M. Chaikin, J. D. Axe, and Y. Fujii, *Phys. Rev. Lett.* **62**:1524 (1989).

18. S. Stoelken, Ph.D. thesis, in progress, Mainz University.
19. W. Schaertl and V. Frenz, Unpublished results.
20. A. Kasper, Ph.D. thesis, in progress, Mainz University.
21. I. Moriguchi, K. Kawasaki, and T. Kawakatsu, to be published.
22. W. Schaertl, Oral presentation, Kyushu University, Fukuoka, Japan (1994).
23. T. G. Fox and P. J. Flory, *J. Appl. Phys.* **21**:581 (1950).
24. G. S. Crest and M. H. Cohen, *Adv. Chem. Phys.* **48**:455 (1981).